CREX
Experimental Results

2023 JLab User Group
Annual Meeting

ericking@temple.edu

Jefferson Lab
Exploring the Nature of Matter
U.S. DEPARTMENT OF ENERGY
TEMPLE UNIVERSITY

Experimental Motivation

In general, we'd like to have a much better understanding of the overall nuclear landscape.

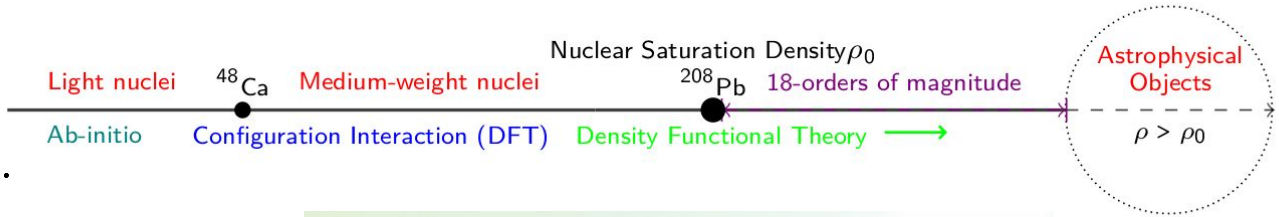

- Ab-initio methods are easily performed for light nuclei
- DFTs are used for medium-weight and heavy-weight nuclei.
- ^{48}Ca lies on the light-to-medium weight nuclei boundary.

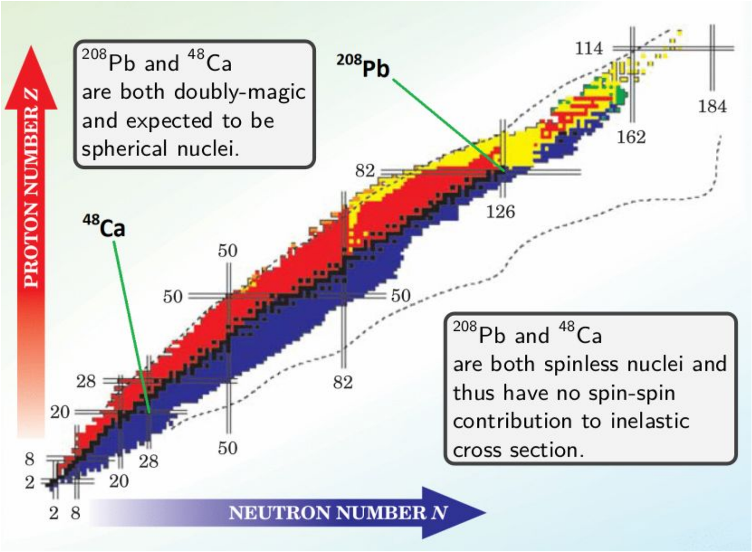

Experimental Motivation

- ^{48}Ca provides a unique opportunity to examine the light-nuclei to medium/heavy-nuclei transitional region to compare to theory.
  - Made it an ideal sister-experiment to PREX-2

- Like ^{208}Pb, ^{48}Ca is doubly-magic meaning that there is no spin-spin correction for the Mott cross-section, simplifying the experiment.

$$\frac{d\sigma}{d\Omega}_{\text{Mott}} = \underbrace{\frac{4\alpha^2 E^2}{|q|^4}\cos^2\frac{\theta}{2}}_{\text{Spin-less Interaction}} - \underbrace{\frac{4\alpha^2 E^2}{|q|^4}\frac{|q|^2}{2M^2}\sin^2\frac{\theta}{2}}_{\text{Spin-spin Interaction Correction}}$$

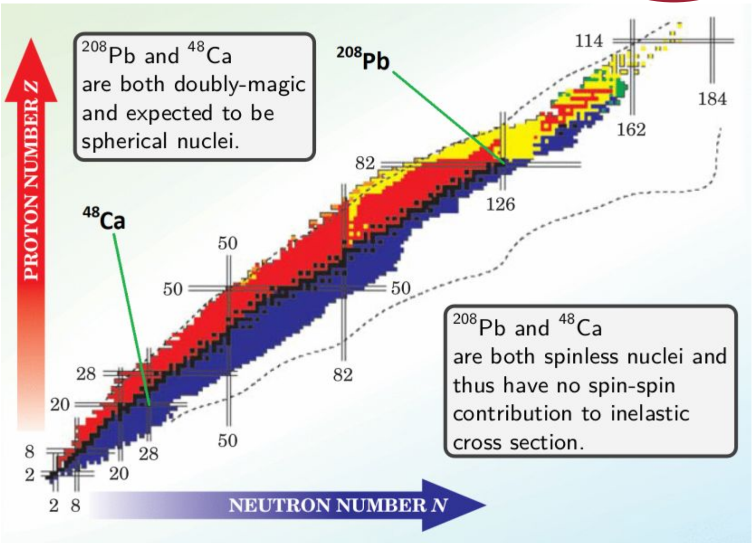

Typical Electron-Nucleon Scattering Experiments

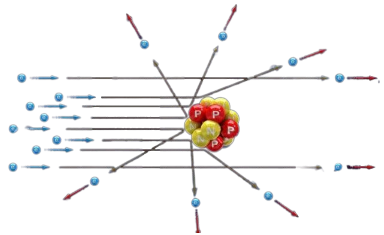

$$F(Q^2) = \int e^{-iq\cdot r}\rho(r)d^3r$$

⟵ Form factors contain information about the charge distribution. They arise from the scattering potential.

$$\frac{d\sigma}{d\Omega} = \frac{d\sigma}{d\Omega}_{\text{Mott}}|F(Q^2)|^2$$

⟵ Act as a modification of the cross section. off a point-like scattering target.

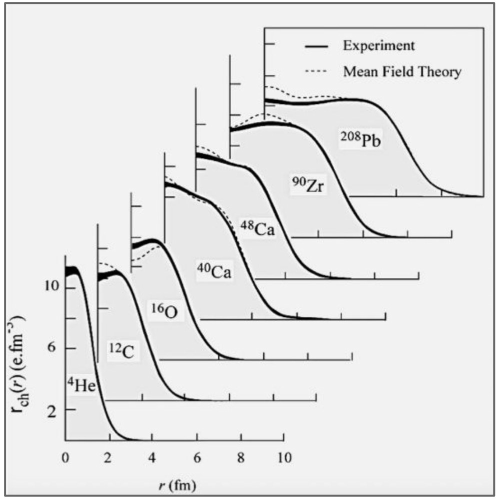

$$F(Q^2) \approx F(0) + Q^2\frac{dF}{dQ^2}|_{Q^2=0} + \ldots$$

$$F(Q^2) \approx \int \rho(\vec{x})d^3x - \frac{1}{6}Q^2 < r^2_{\text{charge}} > + \ldots$$

Cross sections are related to form factors and the valuable physics can be extracted. In this case, charge radii of various nuclei.

EW Implications: Particle Charges

Electromagnetic and Weak Charges of Particles

Particle	Q_e	Q_W
Proton	+1	~0.07
Neutron	0	~1
Electron	-1	$-(1 - 4\sin^2\theta_W)$

Note: Conventionally, this matter is discussed with weak charge; however, the basis for the parity violation is the weak-isospin T_3 which =0 for all right-handed spin states

Image source: QWeak Collaboration

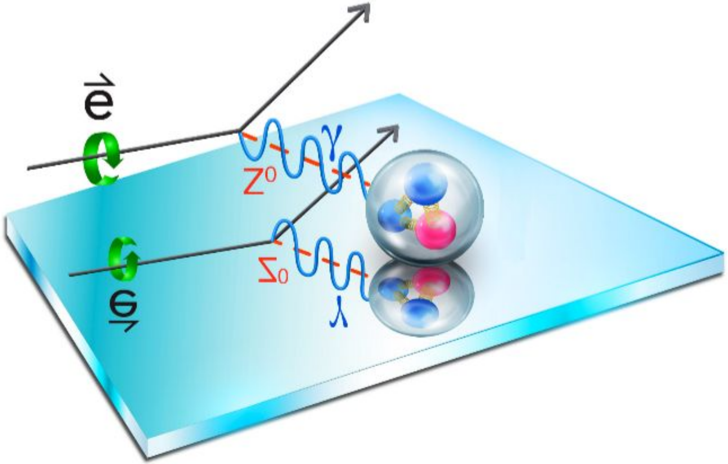

1. Electromagnetic scattering from nucleus only happens with protons.
2. Weak scattering primarily occurs from neutrons and violates parity.

⇒ With the right type of experiment and facility one can take advantage of this phenomenon.

JLab Polarized Source

- Circularly polarized laser incident on superlattice GaAs photocathode.
- Finely tuned and rapidly alternated through use of a RTP Pockel
- Produces bunches of polarized (~90%) electrons.
- Slow noise controlled by alternating usage of insertable halfwave plate.
- Wein flips used for additional control

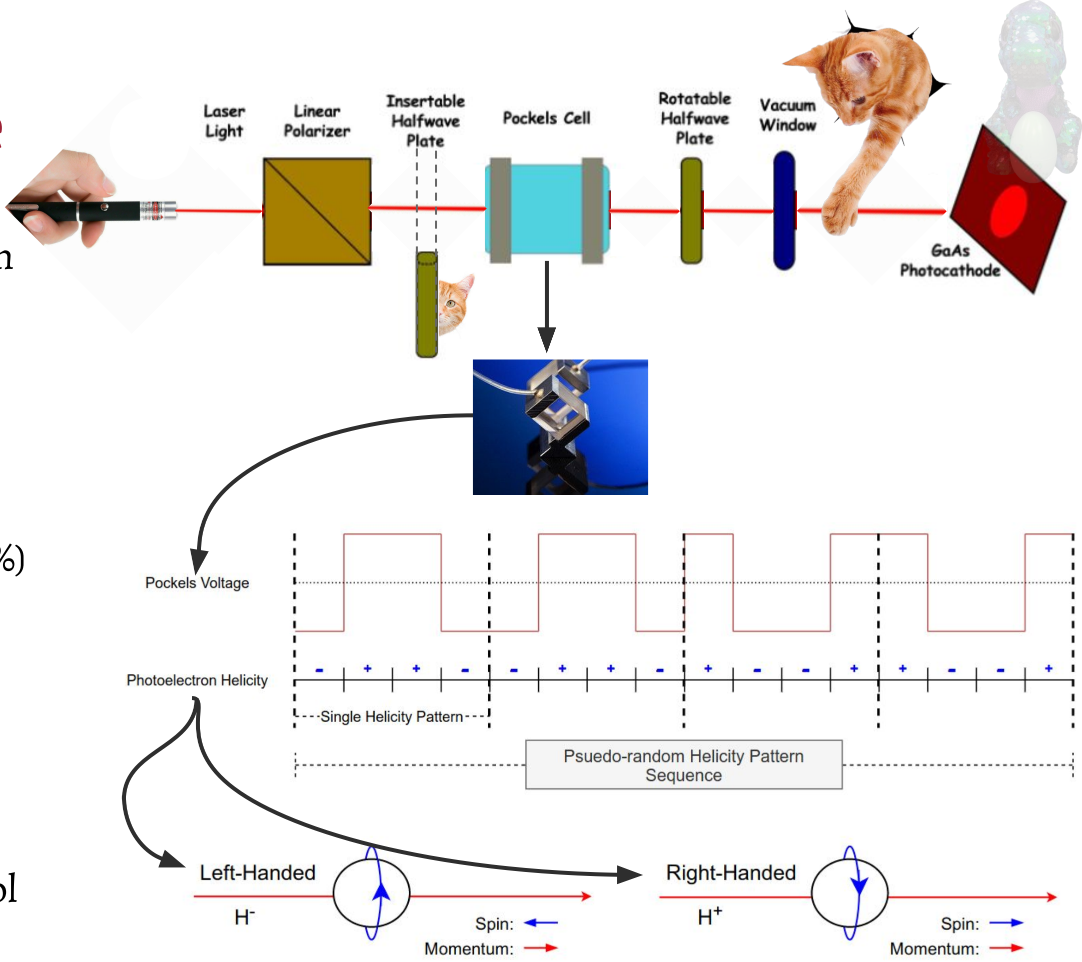

Parity-violating Asymmetry A_{PV}

- Electroweak cross section
  - Account for Gamma and Z_0
- Interference term responsible for parity-violating asymmetry
- $[1 - 4\sin^2\theta_W] \approx 0 \Rightarrow \sin^2\theta_W \sim 0.23xx$
- $F_{CH}(q) \Rightarrow$ Experimentally well-known values
- Measuring the parity-violating asymmetry provides us with a clean way of measuring $F_W(q)$

$\sigma \sim$

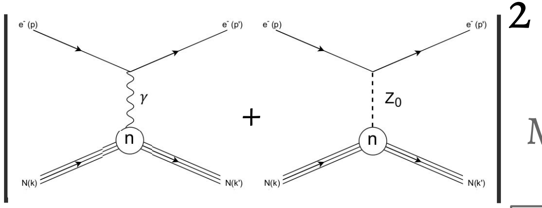

$M_{W,L} = -M_{W,R}$

Note:

$$\sigma \propto |M_\gamma + M_W|^2 = |M_\gamma|^2 + \underbrace{2M_\gamma M_W^*}_{\text{Interference Term}} + |M_W|^2$$

$$A_{PV} = \frac{\sigma_R - \sigma_L}{\sigma_R + \sigma_L} \longrightarrow A_{PV} \approx \frac{2M_\gamma M_W}{M_\gamma^2}$$

$$A_{PV} = \frac{\sigma_R - \sigma_L}{\sigma_R + \sigma_L} \approx \frac{G_F Q^2 |Q_W|}{4\sqrt{2}\pi\alpha Z}\left[1 - 4\sin^2\theta_W - \frac{F_W(Q^2)}{F_{CH}(Q^2)}\right] \approx 10^{-6}$$

$$A_{PV} \approx \frac{G_F Q^2 |Q_W|}{4\sqrt{2}\pi\alpha Z}\frac{F_W(Q^2)}{F_{CH}(Q^2)} \approx 10^{-6}$$

HRS

- HRS – Double Arm Spectrometer
- Capable of precision energy measurement with its native vertical drift chambers
- Captured very small cross section
- QQDQ Optics Setup

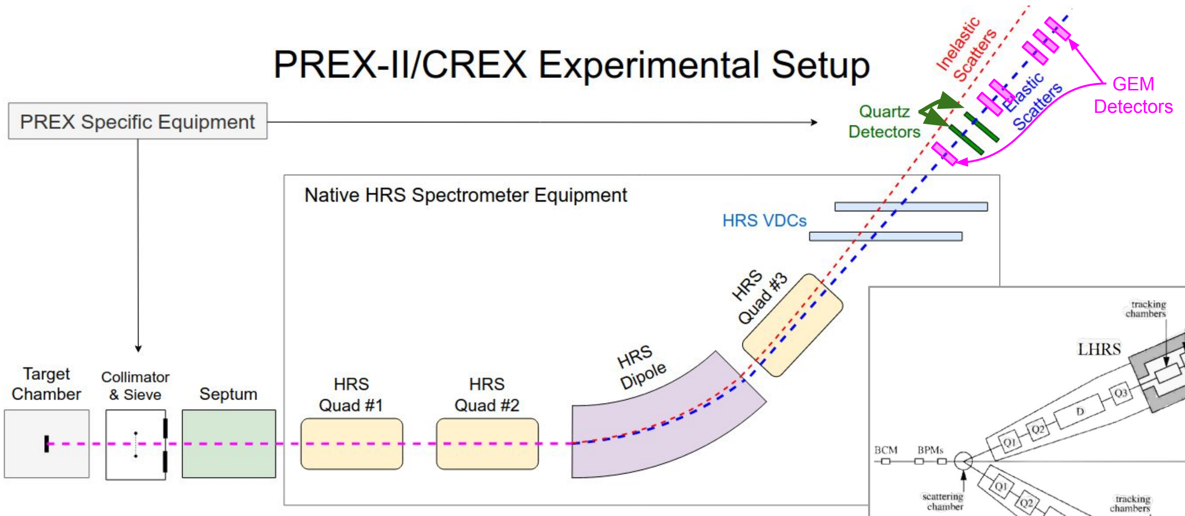

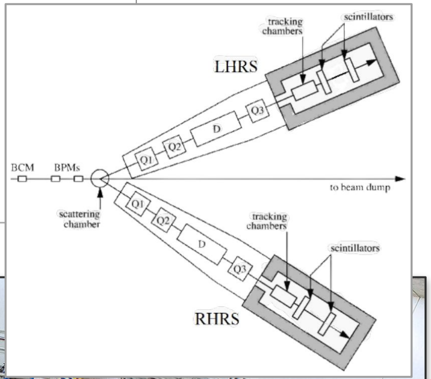

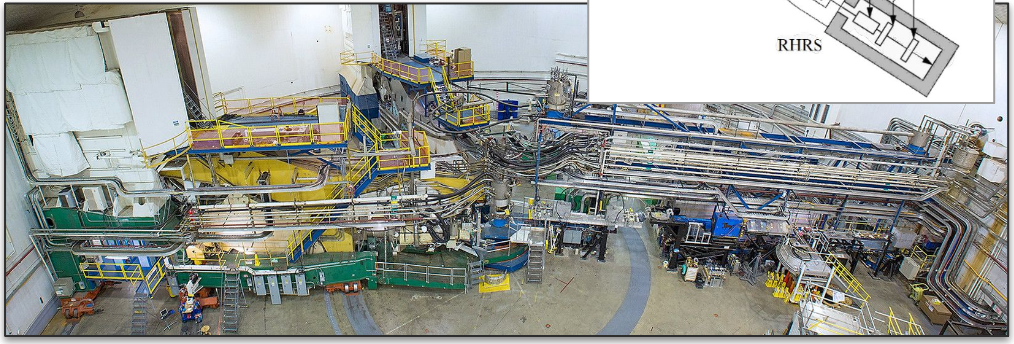

Hall A HRS

- QQDQ Optics Setup
- Optics finely-tuned to separate inelastic scatters out of the detector acceptance.
- Primary collimation immediately after the target scattering defines experimental acceptance.
- Septum magnets bend target scatters from 5° to 12.5° (HRS minimum angle).

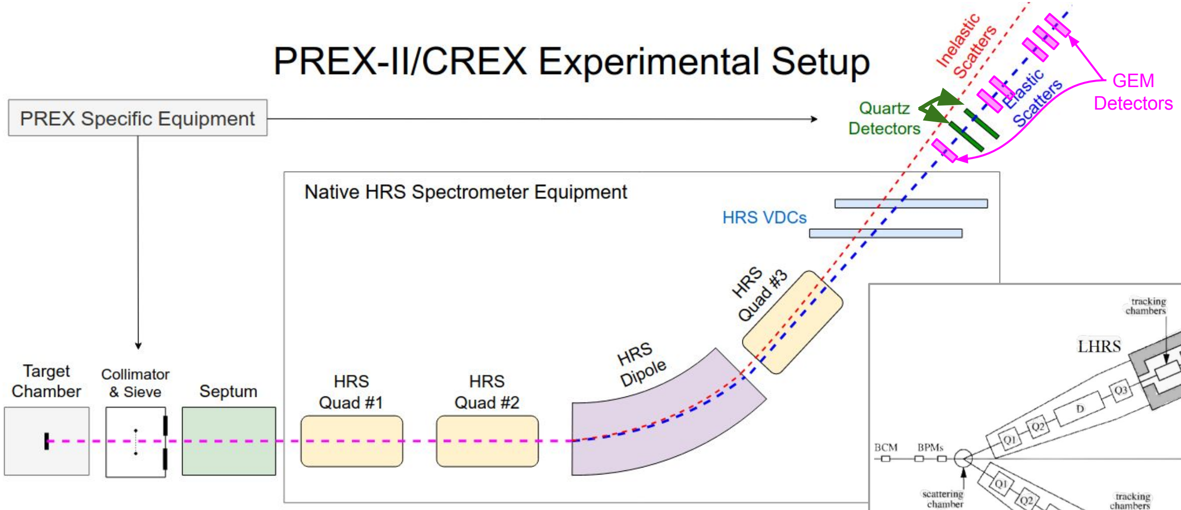

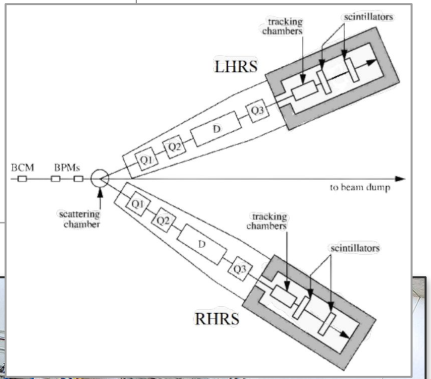

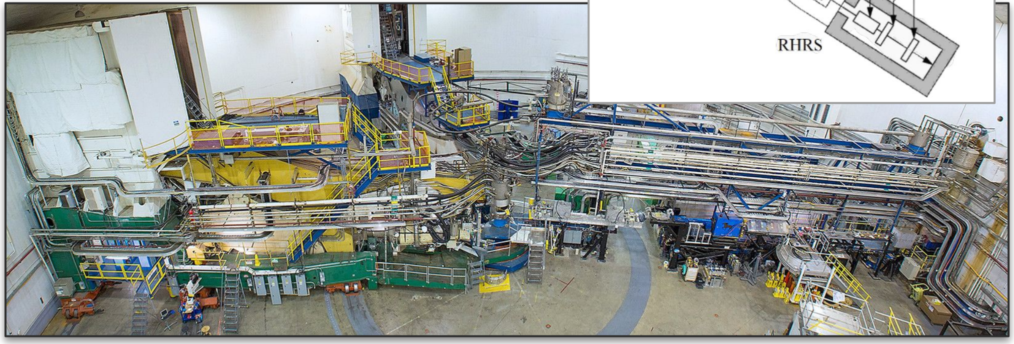

PREX2/CREX Detectors

<u>Quartz Detectors</u>

- Integrating Detectors
- Capable of handling GHz rates
  - CREX
    ~ 50MHz
  - PREX-2
    > 2GHz
- Made of 5mm thick radiation hard silica.

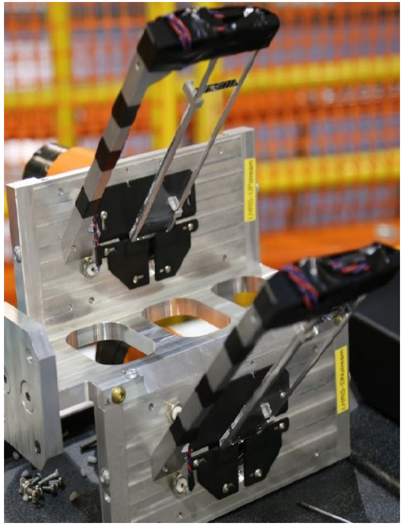

- Each quartz detector connected to PMT

<u>GEM Detectors</u>

- Gaseous Electron Multiplier
- Counting Detector
  - Can identify single MIPs
  - Multiple GEMs can offer effective track reconstruction

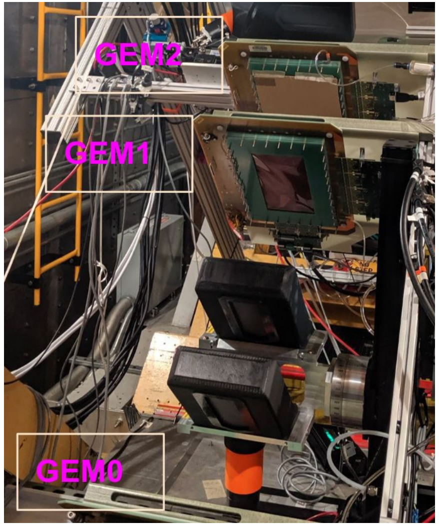

- Used for kinematics measurements and elastic signal alignment.

CREX ^{48}Ca Targets

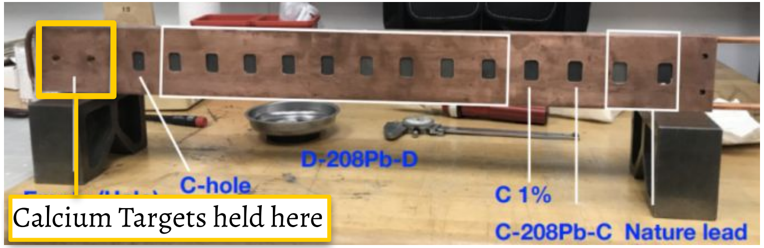

PREX2/CREX Target Ladder

Started with:

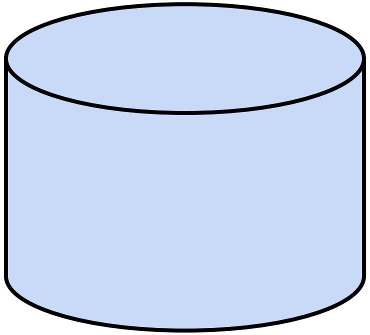

- Single Puck
- 5mm thick
- 96% ^{48}Ca
- 3.48% ^{40}Ca

➢ Enriched 48Ca target

CREX ^{48}Ca Targets

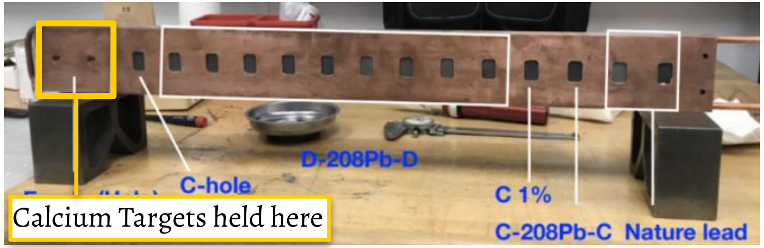

PREX2/CREX Target Ladder

Started with:

- Single Puck
- 5mm thick
- 96% ^{48}Ca
- 3.48% ^{40}Ca

➢ Enriched 48Ca target

🔥 **Beam struck target ladder and destroyed first target**

Ended with:

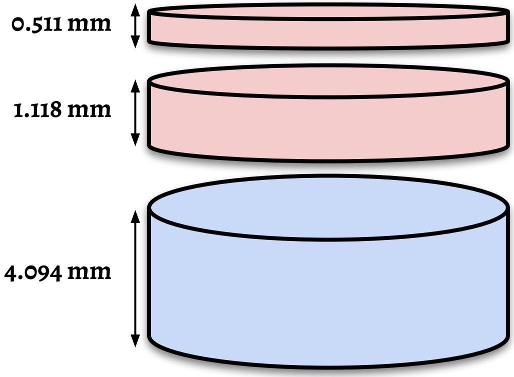

- 1 Puck + 2 foils sandwiched together
- ~91.7% ^{48}Ca
- ~7.96% ^{40}Ca
- ~5.7mm thick

➢ Replacement target

Beam Corrections & Scattering Angle/Water Cell

Beam corrected for position fluctuations, charge asymmetry and energy fluctuations (all of which are continually monitored).

Corrections determined through careful analysis of controlled alterations (a.k.a. "beam modulation") and regression techniques on natural beam jitter.

$$A = A_{raw} - A_Q - \sum \beta_i \Delta x_i - \beta_E A_E$$

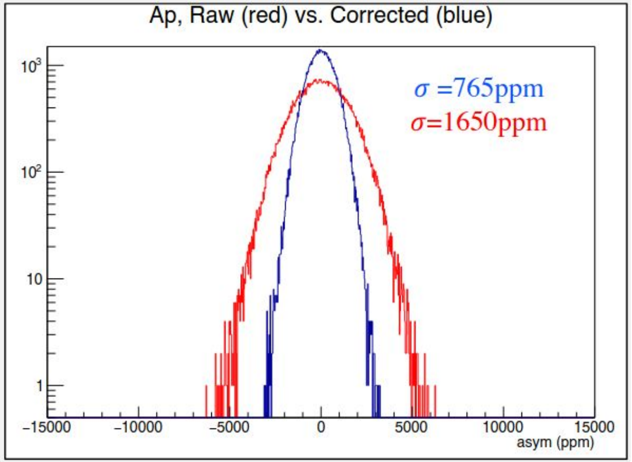

➢ Recoil momentum difference ⇒ Q^2

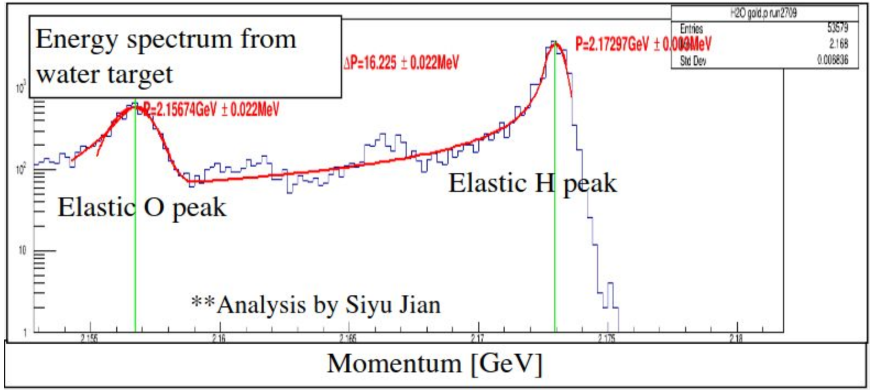

$$\Delta E' = E'_O - E'_H = E\left(\frac{1}{1+\frac{2E\sin^2(\frac{\theta}{2})}{m_O}} - \frac{1}{1+\frac{2E\sin^2(\frac{\theta}{2})}{m_H}}\right)$$

$$Q^2 = 2EE'(\sin^2\frac{\theta}{2}) \longrightarrow A_{PV} \approx \frac{G_F Q^2 |Q_W|}{4\sqrt{2}\pi\alpha Z}\frac{F_W(Q^2)}{F_{CH}(Q^2)} \approx 10^{-6}$$

Beam Polarimetry | Compton + Moller

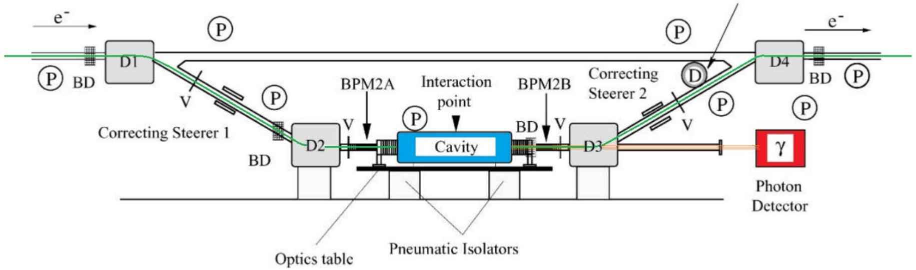

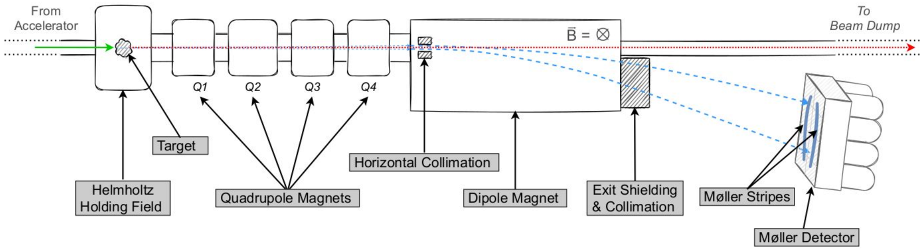

- Compton eγ scattering.
- Electron beam diverted from main beam line into chicane and into circularly polarized light amplified in optical cavity.
- Backscattered γ detected by photon detector
- Minimally destructive to beam and can be run concurrent to experiment.

- Brute force polarimeter.
  - Superconducting magnet holds 4T field to align foil spins in beam direction.
  - ~8% foil polarization
- Looks for Moller coincidence.
- Monte carlo used to determine analyzing power.
- Destructive to beam quality.

Compton Result

87.10% +/- 0.52%

Combined Result

87.09 +/- 0.44%

Moller Result

87.06 +/- 0.85%

*Beam polarization is the largest systematic uncertainty so it's important to get this precise and correct.

Asymmetry Extraction

$$A_{phys} = R_{radcorr} R_{accept} R_{Q^2} \frac{A - P_L \sum_i f_i A_i}{P_L \left(1 - \sum_i f_i\right)}$$

$$A_{corr} = A_{det} - A_{beam} - A_{trans} - A_{nonlin} - A_{blind}$$

The final asymmetry is corrected for:

- $R_{radcorr}$: Radiative Corrections
- R_{accept}: Acceptance
- $R_{Q}2$: Scaling for Q^2
- P_L: Beam Polarization
- $P_L \Sigma_i f_i A_i$: Backgrounds
- A_{corr}: Corrected Asymmetry
- A_{beam}: Beam Corrections
- A_{trans}: Transverse asymmetry correction
- A_{nonlin}: Detector non-linearities
- A_{blind}: Experimental blinding

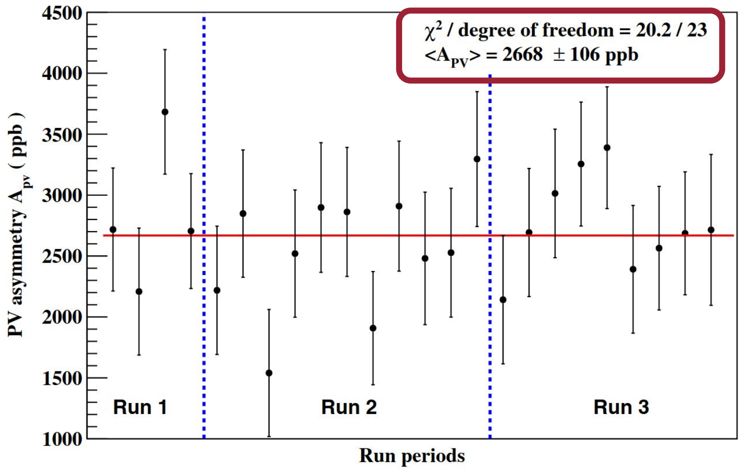

A_{PV} = 2668 ppb + 106 ppb (4.0%) + 40 ppb (1.5%)

Uncertainties

- Dominated by statistical uncertainty 4%
- Beam polarization uncertainty is the largest contributor.
- Beam trajectory/energy uncertainty reasonably well-controlled during experiment
  - Regression/Beam Mod
  - Charge Feedback
- Transverse asymmetry comes from separate measurements.
- Acceptance function uncertainty derived from Monte Carlo

*Table taken from CREX paper.

Correction	Absolute (ppb)	Relative (%)
Beam polarization	382 ± 13	14.3 ± 0.5
Beam trajectory and energy	68 ± 7	2.5 ± 0.3
Beam charge asymmetry	112 ± 1	4.2 ± 0.0
Isotopic purity	19 ± 3	0.7 ± 0.1
3.831 MeV (2^+) inelastic	-35 ± 19	-1.3 ± 0.7
4.507 MeV (3^-) inelastic	0 ± 10	0 ± 0.4
5.370 MeV (3^-) inelastic	-2 ± 4	-0.1 ± 0.1
Transverse asymmetry	0 ± 13	0 ± 0.5
Detector nonlinearity	0 ± 7	0 ± 0.3
Acceptance	0 ± 24	0 ± 0.9
Radiative corrections (Q_W)	0 ± 10	0 ± 0.4
Total systematic uncertainty	40 ppb	1.5%
Statistical uncertainty	106 ppb	4.0%

A_{PV} = 2668 ppb + 106 ppb (4.0%) + 40 ppb (1.5%)

Results: Difference of Form Factors (Main Result)

After the extraction of F_W from A_{PV}

Difference of the charge form factor and weak form factors

- Form factors do vary as a function as a function of Q^2
- F_{ch} is an experimentally well-vetted quantity
- Statistical error shown in black and total experimental error shown in red.

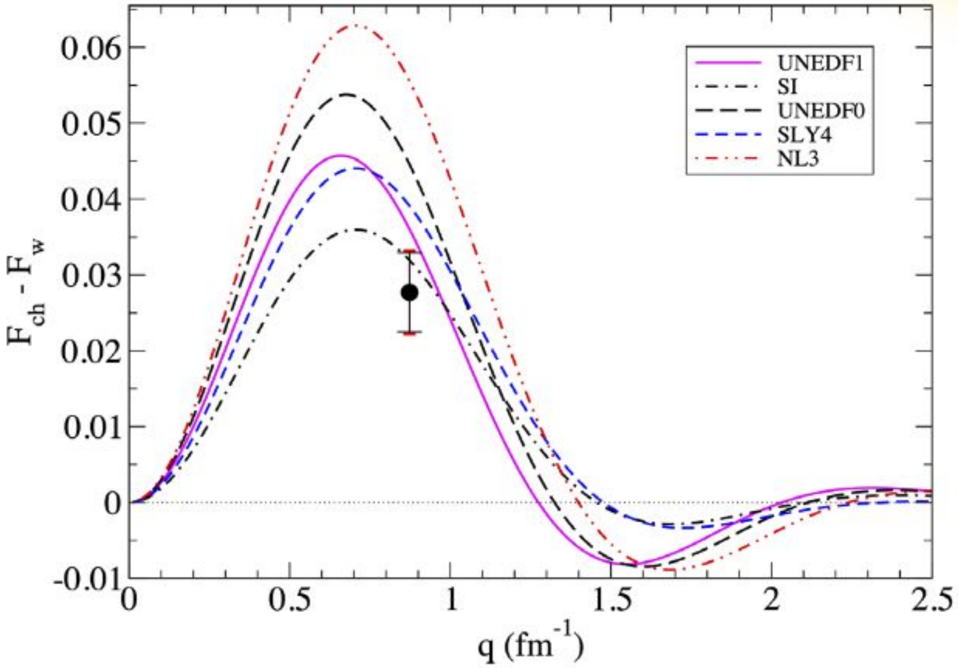

Results: Weak Skin and Neutron Skin

Difference of the charge and weak form factors of ^{48}Ca plotted against R_W-R_{ch} and the ^{48}Ca neutron skin R_{np}

- Extraction of R_W-R_{CH} from F_{CH}-F_W does introduce some model dependence due to Q^2-dependence

- Extraction of R_{np} introduces some additional model differences in relativistic vs. non-relativistic models due to spin orbit $\vec{L} \cdot \vec{S}$ dependencies.

Relativistic density functional models shown in **magenta diamonds** while non-relativistic are shown in **gray circles**.

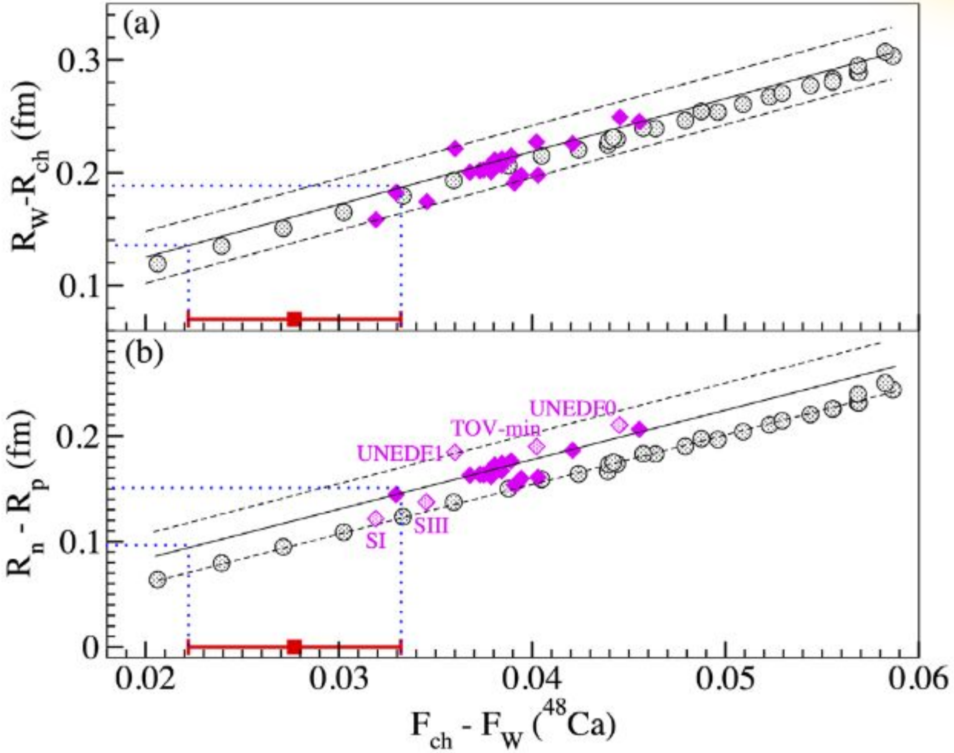

Results: CREX & PREX2 Neutron Skin

CREX results and PREX-2 neutron skin results plotted against

- The results are consistent at the 90% level with several DFT models.
- The combined CREX/PREX2 results are consistent with the coupled cluster mode.

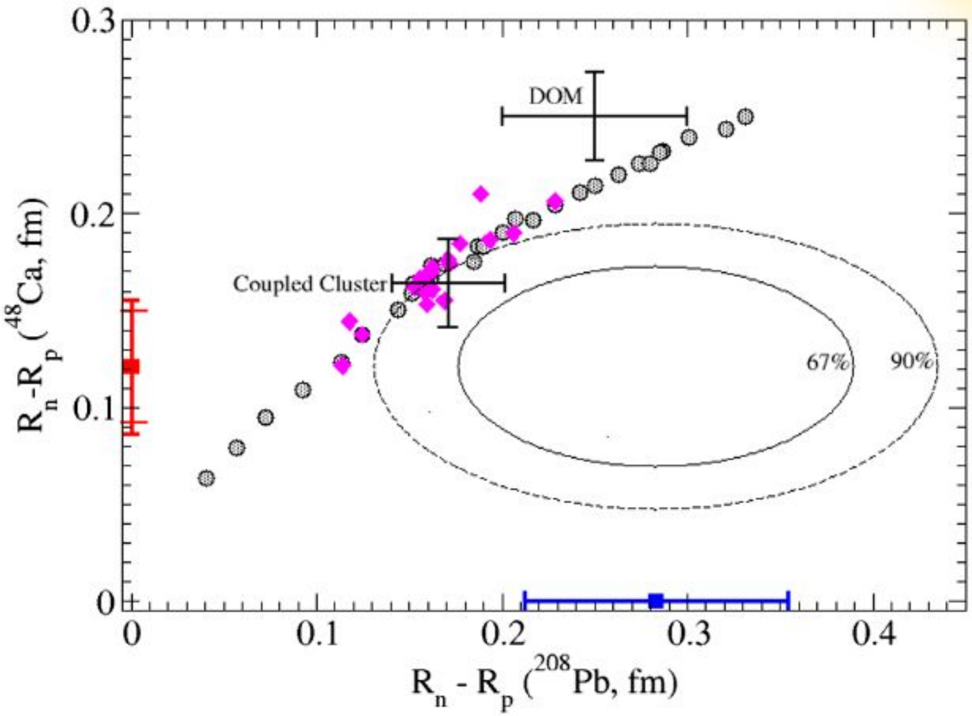

Conclusions

- 48Ca has a thinner neutron skin than predicted by models.
  - As a reminder, PREX2 revealed results that correlate to a thicker than expected neutron skin.
- Combined with the PREX2 measurements the precision CREX result provides additional and valuable information for predicting neutron skin of nuclei.
  - Helps bridge the divide between ab-initio calculations and DFT predictions in the light- to medium-weight nuclei.

Acknowledgements / Questions / Comments

The CREX Collaboration

PHYSICAL REVIEW LETTERS **129**, 042501 (2022)

Editors' Suggestion

Precision Determination of the Neutral Weak Form Factor of ^{48}Ca

D. Adhikari,[1] H. Albataineh,[2] D. Androic,[3] K. A. Aniol,[4] D. S. Armstrong,[5] T. Averett,[5] C. Ayerbe Gayoso,[5] S. K. Barcus,[6] V. Bellini,[7] R. S. Beminiwattha,[8] J. F. Benesch,[6] H. Bhatt,[9] D. Bhatta Pathak,[8] D. Bhetuwal,[9] B. Blaikie,[10] J. Boyd,[11] Q. Campagna,[5] A. Camsonne,[6] G. D. Cates,[11] Y. Chen,[8] C. Clarke,[12] J. C. Cornejo,[13] S. Covrig Dusa,[6] M. M. Dalton,[6] P. Datta,[14] A. Deshpande,[12,15,16] D. Dutta,[9] C. Feldman,[12,17] E. Fuchey,[14] C. Gal,[15,9,11,12] D. Gaskell,[6] T. Gautam,[18] M. Gericke,[10] C. Ghosh,[19,12] I. Halilovic,[10] J.-O. Hansen,[6] O. Hassan,[10] F. Hauenstein,[6] W. Henry,[20] C. J. Horowitz,[21] C. Jantzi,[11] S. Jian,[11] S. Johnston,[19] D. C. Jones,[20,6] S. Kakkar,[10] S. Katugampola,[11] C. Keppel,[6] P. M. King,[22] D. E. King,[23,20] K. S. Kumar,[19] T. Kutz,[12] N. Lashley-Colthirst,[18] G. Leverick,[10] H. Liu,[19] N. Liyanage,[11] J. Mammei,[10] R. Mammei,[24] M. McCaughan,[6] D. McNulty,[1] D. Meekins,[6] C. Metts,[5] R. Michaels,[6] M. Mihovilovic,[25,26] M. M. Mondal,[12,15] J. Napolitano,[20] A. Narayan,[27] D. Nikolaev,[20] V. Owen,[5] C. Palatchi,[11,15] J. Pan,[10] B. Pandey,[18] S. Park,[9,12] K. D. Paschke,[11,*] M. Petrusky,[12] M. L. Pitt,[28] S. Premathilake,[11] B. Quinn,[13] R. Radloff,[22] S. Rahman,[10] M. N. H. Rashad,[11] A. Rathnayake,[11] B. T. Reed,[21] P. E. Reimer,[29] R. Richards,[12] S. Riordan,[29] Y. R. Roblin,[6] S. Seeds,[14] A. Shahinyan,[30] P. Souder,[23] M. Thiel,[31] Y. Tian,[23] G. M. Urciuoli,[32] E. W. Wertz,[5] B. Wojtsekhowski,[6] B. Yale,[5] T. Ye,[12] A. Yoon,[33] W. Xiong,[23,34] A. Zec,[11] W. Zhang,[12] J. Zhang,[12,15,34] and X. Zheng[11]

Participating Institutions

[1]*Idaho State University, Pocatello, Idaho 83209, USA*
[2]*Texas A & M University—Kingsville, Kingsville, Texas 78363, USA*
[3]*University of Zagreb, Faculty of Science, Zagreb, HR 10002, Croatia*
[4]*California State University, Los Angeles, Los Angeles, California 90032, USA*
[5]*William and Mary, Williamsburg, Virginia 23185, USA*
[6]*Thomas Jefferson National Accelerator Facility, Newport News, Virginia 23606, USA*
[7]*Istituto Nazionale di Fisica Nucleare, Sezione di Catania, 95123 Catania, Italy*
[8]*Louisiana Tech University, Ruston, Louisiana 71272, USA*
[9]*Mississippi State University, Mississippi State, Mississippi 39762, USA*
[10]*University of Manitoba, Winnipeg, Manitoba R3T2N2, Canada*
[11]*University of Virginia, Charlottesville, Virginia 22904, USA*
[12]*Stony Brook, State University of New York, Stony Brook, New York 11794, USA*
[13]*Carnegie Mellon University, Pittsburgh, Pennsylvania 15213, USA*
[14]*University of Connecticut, Storrs, Connecticut 06269, USA*
[15]*Center for Frontiers in Nuclear Science, Stony Brook, New York 11794, USA*
[16]*Brookhaven National Laboratory, Upton, New York 11973, USA*
[17]*Institute for Advanced Computational Science, Stony Brook, New York 11794, USA*
[18]*Hampton University, Hampton, Virginia 23668, USA*
[19]*University of Massachusetts Amherst, Amherst, Massachusetts 01003, USA*
[20]*Temple University, Philadelphia, Pennsylvania 19122, USA*
[21]*Indiana University, Bloomington, Indiana 47405, USA*
[22]*Ohio University, Athens, Ohio 45701, USA*
[23]*Syracuse University, Syracuse, New York 13244, USA*
[24]*University of Winnipeg, Winnipeg, Manitoba R3B2E9, Canada*
[25]*Jožef Stefan Institute, SI-1000 Ljubljana, Slovenia*
[26]*Faculty of Mathematics and Physics, University of Ljubljana, SI-1000 Ljubljana, Slovenia*
[27]*Veer Kunwar Singh University, Ara, Bihar 802301, India*
[28]*Virginia Tech, Blacksburg, Virginia 24061, USA*
[29]*Physics Division, Argonne National Laboratory, Lemont, Illinois 60439, USA*
[30]*A. I. Alikhanyan National Science Laboratory (Yerevan Physics Institute), Yerevan 0036, Armenia*
[31]*Institut für Kernphysik, Johannes Gutenberg-Universität, Mainz 55122, Germany*
[32]*INFN - Sezione di Roma, I-00185 Rome, Italy*
[33]*Christopher Newport University, Newport News, Virginia 23606, USA*
[34]*Shandong University, Qingdao, Shandong 266237, China*

Questions?

Comments.

Publications

Precision Determination of the Weak Form Factor of ^{48}Ca
https://doi.org/10.1103/PhysRevLett.129.042501 arXiv:2205.11593v2

An overview of how parity-violating electron scattering experiments are performed at CEBAF
https://doi.org/10.1016/j.nima.2022.167710 (*open access*)

An Accurate Determination of the Neutron Skin Thickness of ^{208}Pb Through Parity-Violation in Electron Scattering
http://dx.doi.org/10.1103/PhysRevLett.126.172502 arXiv:2102.10767

New Measurements of the Beam-normal Single Spin Asymmetry in Elastic Electron Scattering over a Range of Spin-0 Nuclei
https://doi.org/10.1103/PhysRevLett.128.142501 arXiv:2111.04250

Precision Møller polarimetry for PREX-2 and CREX
https://doi.org/10.1016/j.nima.2022.167506 arXiv:2207.02150

Accurate Determination of the Electron Spin Polarization in Magnetized Iron and Nickel Foils for Møller Polarimetry
https://doi.org/10.1016/j.nima.2022.167444 arXiv:2203.11238

PhD Theses: Devi Adhikari, Cameron Clarke, Tao Ye, Sakib Rahman, Ryan Richards, Robert Radloff, Eric King, Weibin Zhang, Siyu Jian, Amali Premathilake, Allison Zec

Backup Slides

Someone may ask

- Move to backup slide just for reference.

Extracted (and Used) Physics Values

$$Note: \ \mathrm{q} = \sqrt{Q^2}$$

Quantity	Value	(stat)	(sys)
A_{PV}	2668 ppb	106	
$\langle Q^2 \rangle$	0.0297 GeV^2/c^2		
q	0.8733 fm^{-1}		
$F_W(q) / F_{CH}(q)$	0.8428	0.0328	0.0124
$F_{CH}(q)$	0.1581		
$F_W(q)$	0.1304	0.0052	0.0020
$F_{CH}(q) - F_W(q)$	0.0277	0.0052	0.0020
R_W-R_{CH}	0.159	0.026	0.023
R_n-R_p	0.121	0.026	0.024

- Move to backup slide just for reference.

Physics Extraction

After the parity-violating asymmetry is extracted from the data:

- The weak form factor can be extracted.
- From that we can get the weak density and the weak radius.
- Finally the neutron skin can be extracted.

$$A_{PV} \rightarrow F_W \rightarrow \rho_W \rightarrow R_W \rightarrow R_{np}$$

$$A_{PV} \approx \frac{G_F Q^2 |Q_W|}{4\sqrt{2}\pi\alpha Z} \frac{F_W(Q^2)}{F_{CH}(Q^2)} \approx 10^{-6}$$

$$F_W(Q^2) = \frac{1}{4\pi Q_W} \int d^3r\, j_0(Qr)\rho_W(r)$$

$$R_{np} = \left(1 + \frac{Z Q_{W_p}}{N Q_{W_n}}\right)(R_W - R_{ch})$$

The last equation was Chucks formulation in one of his talks for PREX that I used in my thesis; I honestly don't know if this is the same method used here given that there was apparently more model dependence in the neutron skin extraction.

Compton and Møller Measurement Overlay

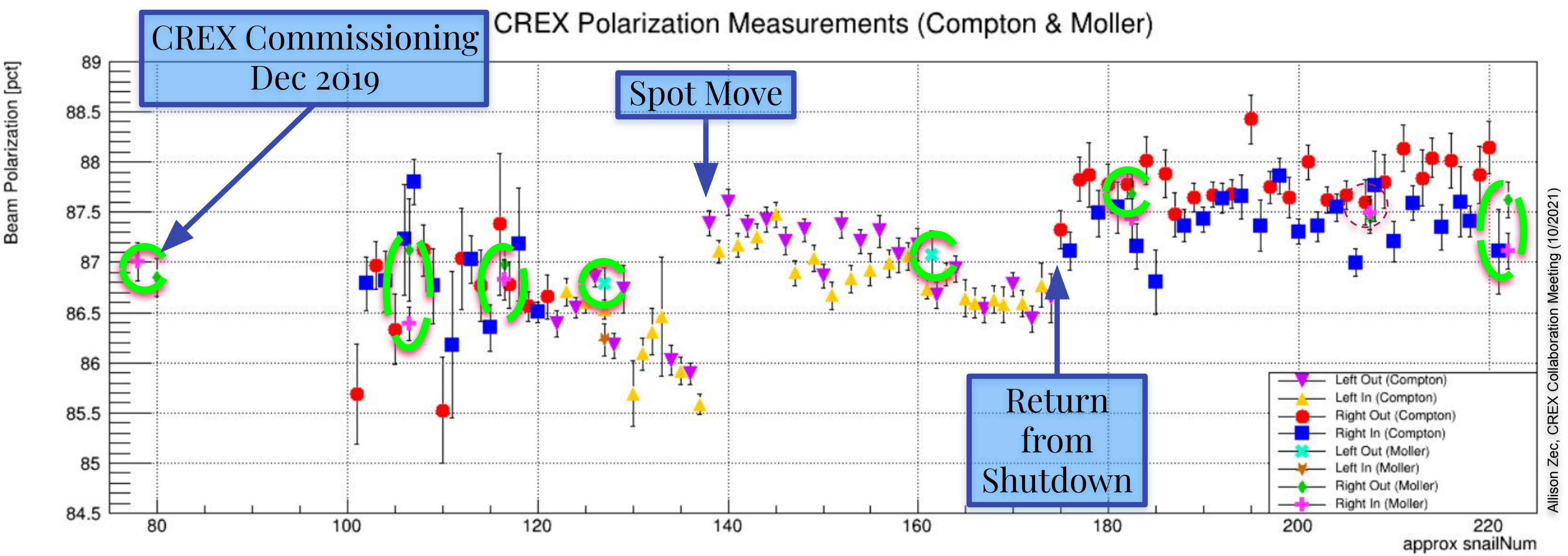

➢ Møller and Compton measurements <u>were consistent</u> throughout the CREX experiment.

I've made an attempt to highlight the less-frequent Moller measurements among the Comptons

Comparison of Compton & Møller Polarization Measurements

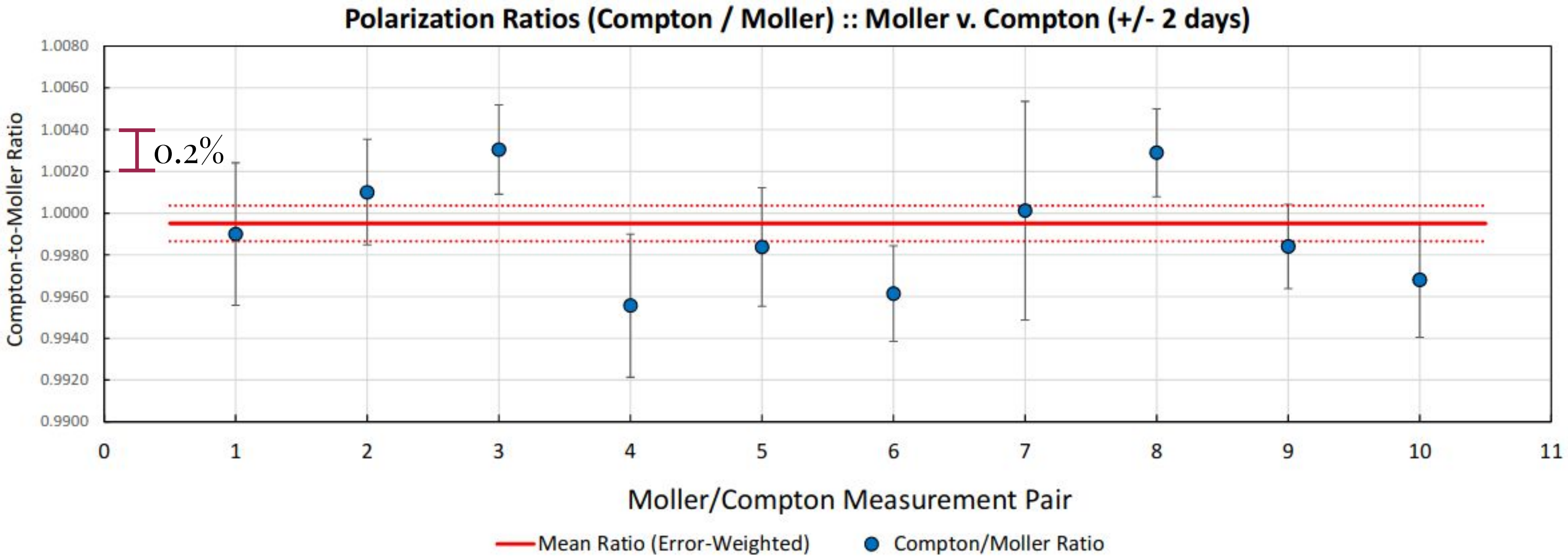

- Møller measurements were compared to Compton measurements taken within roughly ± 48 hours.
- The mean Compton/Møller ratio was **0.9995 ± 0.0008**

  Ratio consistent with 1 at the ~0.1% level.